https://doi.org/10.1016/j.engstruct.2018.03.006

A study of hybrid self-centring connections equipped with shape memory alloy washers and bolts

Cheng Fang[a)], Michael C. H. Yam[b)*], Tak-Ming Chan[c)], Wei Wang[a)], XiaoYang[a)], Xuemei Lin[b)]

[a)] *Department of Structural Engineering, School of Civil Engineering, Tongji University, Shanghai 200092, China*
[b)] *Department of Building & Real Estate, The Hong Kong Polytechnic University, Hung Hom, Kowloon, Hong Kong, China*
[c)] *Department of Civil & Environmental Engineering, The Hong Kong Polytechnic University, Hung Hom, Kowloon, Hong Kong, China*
** Corresponding author: email: michael.yam@polyu.edu.hk, Tel: (852) 2766 4380*

Abstract: This paper presents an innovative type of hybrid self-centring extended end-plate connections incorporating high strength bolts and two basic SMA elements, namely, SMA Belleville washers and SMA bolts. The fundamental mechanical characteristics of the individual SMA elements were first understood via cyclic tests, and subsequently a comprehensive test programme on of four proof-of-concept connections with varying bolt dimensions and washer arrangements was conducted. The connection specimens exhibited flag-shape hysteretic responses with good self-centring ability and cyclic loading repeatability. Satisfactory ductility accompanied by moderate energy dissipation capacity was also shown, and it was found that the SMA washers contributed evidently to the strength, stiffness, and energy dissipation of the connections. A numerical investigation was subsequently performed to enable a more in-depth understanding of the connection behaviour, and it was further shown that increasing the preload levels of either the SMA washers or the SMA bolts could effectively increase the connection stiffness. A design model was finally proposed which enables an idealised bi-linear description of the moment-rotation responses of the hybrid self-centring connections. The design stiffness and strength obtained from the proposed models were found to agree reasonably well with the test results and numerical predictions.

Keywords: shape memory alloy (SMA); extended end-plate connection; self-centring; numerical study.

1. Introduction

Steel moment resisting frames (MRFs) are a prevailing class of lateral load resisting systems for multi-storey and high-rise building structures. They are often deemed to have satisfactory seismic

performance under strong earthquakes, provided that large inelastic deformations with sufficient ductility intentionally occur in specific members such as steel beams [1]. However, the 1994 Northridge and 1995 Kobe earthquakes exposed deficiencies of conventional beam-to-column connections which experienced extensive weld fracture. After these major events, the ductility performance of such connections has been carefully re-visited, and extensive follow-up investigations have been conducted, leading to improved connection design. These post-Northridge prequalified connections, either fully-restrained or partially-restrained, are expected to ensure life safety for the occupants by providing large inelastic rotations while maintaining their strength without significant degradation.

However, the plastic deformations induced at or near these connections are not easily recoverable, and thus permanent residual drifts could remain at the end of seismic excitations. A study conducted by McCormick et al. [2] found it impractical to repair damaged structures when the residual drift is greater than 0.5%. Even if the structures are repairable, decision makers can be faced with a dilemma of whether or not to repair them as the cost of the repair work can be prohibitively high. Moreover, the prolonged suspension of building functions hinders the community to rebound effectively from infrastructure disruption and business downtime. Some critical facilities, such as hospitals, government headquarters, and military facilities, cannot afford even a short occupancy suspension due to their unique purposes of service. Furthermore, multiple earthquakes, e.g., main-shock and aftershock sequences, could result in accumulation of permanent residual deformation [3]. Therefore, earthquake resilient structures which exhibit low levels of residual drifts nowadays become one of the hottest subjects among the community of seismic engineers and researchers. To this end, a novel category of seismic-resisting structures, namely, self-centring structures, has been proposed [4], and among the various available solutions, endowing the beam-to-column connections with self-centring abilities has attracted great attention.

The concept of self-centring connections was first realised by the application of post-tensioned steel tendons, anchored at the external or other selected columns parallel to the steel beams

[5-6]. The self-centring driving force is provided by the connection gap opening that induces elastic elongation of the steel tendons/cables. Meanwhile, the commercial availability of superelastic shape memory alloys (SMAs) motivated researchers to develop alternative solutions for self-centring connections. The 'superelastic effect', which is triggered when the SMA is deformed in the austenitic form, allows the stress-induced deformation (up to 10% strain) to be recovered spontaneously upon unloading, and due to reversible microstructural interfacial motion, hysteresis loops are developed when SMA is under cyclic load [7]. The SMA solution may have the benefits of easy installation, compact size, no extra compression to steel beams, and good corrosion resistance. Some preliminary studies suggested that compared with conventional MRFs, an appropriate arrangement of SMA connections could lead to significantly reduced residual inter-storey drifts and concurrently well controlled peak deformation [1, 8].

As for detailing, Ma et al. [9] proposed a prototype connection type which is modified from conventional extended end-plate connections, where the high-strength bolts were all replaced by SMA bolts. This idea was then verified through an experimental study [10], where good self-centring ability with moderate energy dissipation was shown. However, the shear resistance of these connections was solely provided by the friction between the end-plate and column face, a mechanism which is unreliable under large shear forces [11]. Penar [12] and Speicher *et al*. [13] performed a series of proof-of-concept tests on shear tab steel connections with external SMA bolts. Satisfactory hysteretic behaviour with improved shear resistance was seen, but the issues of installation complexity and floor-slab interference were not adequately considered in the study. In addition, the torque applied to the shear tab bolts induced friction which had detrimental influence on the self-centring performance. Some researchers attempted to add low yield strength steel angles to increase the energy dissipation of SMA-based connections [14-16], and the test results showed that this had to be realised at the cost of increased residual deformation. Other proof-of-concept SMA connections including innovative SMA components (e.g. SMA ring springs) are also under investigation [17-20].

In this paper, a new type of self-centring connection, namely, hybrid self-centring connections with high strength bolts, SMA Belleville washers and SMA bolts (abbreviated as SMA-WB connections), is proposed. The development of this connection type is inspired by the aforementioned SMA-based extended end-plate connections, but is modified to enable a more appropriate load resisting mechanism. In the following discussions, the key properties of the two SMA elements used for the connection, i.e., SMA Belleville washers and SMA bolts, are introduced first. After understanding their basic mechanical characteristics, proof-of-concept SMA-WB connections are physically tested, which is followed by a detailed numerical investigation. Design comments on such connections are finally made, and analytical models are also developed to facilitate practical design.

2. Basic characteristics of key SMA elements

2.1 Concise principle of SMA-WB connections

As schematically illustrated in Fig. 1(a), the proposed SMA-WB connections typically include a series of external SMA bolts and sets of SMA Belleville washers for the internal bolt row. The external SMA bolts are mainly used to provide moment resistance as well as self-centring driving force. Standard high strength (HS) bolts, which are used in conjunction with the SMA Belleville washer sets, are employed for the internal bolt row. The shear resistance of the connection is mainly provided by the HS bolts, and in addition, aided by the friction between the end-plate and the column face. The SMA Belleville washers are used to offer a certain level of rotational flexibility for the HS bolts and concurrently to promote self-centring and energy dissipation. With this arrangement, the deformation of the internal bolt row during loading is mainly provided by the SMA Belleville washers and, hence, minimises any permanent deformation that may occur in the HS bolts. The proposed SMA-WB connections can also have minimal spatial interference with the adjacent structural members such as the minor axis beam-to-column connections. Moreover, the installation procedure is similar to that used in conventional end-plate connections.

2.2 SMA Belleville washers

Belleville washers, also known as disc springs and sometimes simplified as washers, are traditional mechanical components that can be used with different stack patterns to provide different combinations of load resistance and deformability. As shown in Fig. 1(a), the governing geometric parameters for a Belleville washer include the external diameter (D_e), internal diameter (D_i), height (H), thickness (T), as well as cone angle (θ). A group of Belleville washers can be stacked in series or in parallel, where the former combination leads to increased deformability but unchanged resistance, whereas the latter one results in increased load resistance but unchanged deformability. The annular conical shape of Belleville washers enables relatively stable and concentric force transmissions with small installation space required.

By endowing Belleville washers with superelastic properties, much larger recoverable deformations accompanied by hysteretic damping could be promoted, and, as a result, the application can be further broadened. In fact, the idea of SMA Belleville washers (hereafter simplified as SMA washers) had been implemented by researchers since the 1990s, where the main focus at that time was given to their applications in the field of electrical engineering [21]. The thermo-mechanical producing process for SMA washers was discussed by Maletta et al. [22]. A more relevant study carried out by Speicher et al. [23] showed that the damping performance of SMA washers could be unsatisfactory due to an inappropriate design of the cone angle. By conducting a series of numerical investigations, some recommendations on the key geometric parameters have been proposed [24], based on which a representative SMA washer, with the dimension marked in Fig. 1(a), was designed for the current study. The superelastic SMA washers were directly ordered from the supplier SAES Smart Materials (www.memry.com). Per information from the supplier, the composition of the washers was 55.87% nickel by weight with the remaining contributed by titanium. Each washer had a maximum deformation capacity (H_0) of approximately 2.7 mm. The typical cyclic test result at room temperature (23 ℃) is given in Fig. 1(b), showing satisfactory self-centring ability, repeatability, and energy dissipation capacities. Details of the test arrangement for the individual washers can be found

elsewhere [24]. A consistent geometrical configuration was considered for all the SMA washers used in the current test programme.

2.3 SMA bolts

A uniaxial bar is one of the most widely considered forms of SMA products due to its high material utilisation efficiency. Through extensive investigations since the 1990s, the cyclic performance of individual SMA bars is nowadays well understood. For structural engineering applications, SMA raw bars are often machined into the bolt form. In this study, two nominal bolt shank diameters, namely, D_1 = 8 mm and D_1 = 12 mm, were considered. For the 8 mm diameter bolts, the total bolt length (L) is 240 mm or 290 mm; and for the 12 mm diameter ones, a consistent L of 290 mm is employed. Details of the bolt geometric configuration are given in Fig. 1(a) and Table 1. The SMA bolts were machined from commercial superelastic raw bars, which were purchased from the same material supplier (i.e., SAES Smart Materials) with the same composition as that of the SMA washers. Material coupon tests were conducted on typical 8 mm-diameter SMA bolts, and the hysteretic stress-strain response at room temperature is given in Fig. 1(b). The material test stopped due to the limitation of the capacity of the tensile machine.

From a practical application point of view, one common issue for SMA bolts is their threaded ends which can be quite susceptible to fracture over the net area. A number of previous studies showed that a net threaded-to-shank diameter ratio (D_3/D_1 ratio) of approximately 1.0 is generally inadequate and often leads to early bolt fracture [10, 25]. Ensuring a sufficient D_3/D_1 ratio of the SMA bolts is an effective way to prevent premature fracture over the threaded area. The tests conducted by Speicher et al. [13] confirmed that an increased D_3/D_1 ratio of 1.4 is adequate to avoid bolt fracture, but this is at the cost of increased material waste during the machining process. In other words, the practical D_3/D_1 ratio should neither be too low, nor too high. Based on the limited test data, it was decided to take nominal D_3/D_1 ratios of 1.25 and 1.30 for the current 8 mm and 12 mm diameter bolts, respectively. With this detailing, none of the bolts experienced fracture during the entire testing procedure.

3. Connection test program

3.1 Test specimens

A total of four proof-of-concept connection specimens were tested. These specimens were small-scale connections for concept verification purposes, and they were not designed based on any prototype building. Each specimen consisted of a S355 H150×100×10×10 built-up steel beam, a S355 H350×350×16×24 built-up steel column, and the associated connection zone including the beam stiffeners. The sizes of the steel beam and column were selected based on the concept that the inelastic rotation occurs in the connection zone, with the beam and column being elastic. The total length of the steel beam was 1.15 m, which is sufficiently long to capture the overall bending behaviour of the specimens, but is suitably short for applying a reasonable level of shear force onto the connection. The steel column was deliberately oversized for repeatable use, and as a result, the deformation of the column (including the shear deformation of the panel zone) is assumed negligible. Tension coupon tests [26] were performed to obtain the material properties of the steel members, where the measured values are given in Table 2. The basic properties of the SMA washers and bolts have been discussed in Section 2.

Among the four connection specimens, three were designed as SMA-WB connections. For comparison purposes, the remaining specimen was equipped with SMA bolts only. The main test parameters are SMA bolt length, SMA bolt diameter, and SMA washer arrangement. Each SMA-WB connection had three bolt rows, i.e., two external SMA bolt rows and one internal HS bolt row, and as aforementioned, the internal HS bolts, which provide shear resistance, were used in conjunction with the SMA washers. To allow different SMA bolt lengths to be considered, specially designed steel blocks with different sizes were employed for the SMA bolt rows, as shown in Fig. 1(a). It should be noted that in practice, these blocks may be unnecessary as the SMA bolts may conveniently pass through the column depth. For the remaining specimen with SMA bolts only, the internal HS bolt row was removed, and the shear resistance of the connection had to be provided by the friction between the end-plate and the column face. In case of insufficient shear resistance, which might

damage the specimen as well as the testing facility, additional stoppers were welded at the column face for this specimen.

For easy identification, each specimen was designated according to the bolt size and SMA washer arrangement. The designation starts with the SMA bolt shank diameter (D8 or D12), followed by the total length of the bolt (L240 or L290), and ends with the washer arrangement (W8 and W16). For the washer arrangement, in particular, W8 and W16 indicate the total number of washers employed for each specimen, i.e., 4 washers per bolt and 8 washers per bolt, respectively. For the case of W8, four washers were stacked in series for each HS bolt, and this pattern provides a total deformation capacity of approximately 10.8 mm. For the case of W16, four pairs of washer group were stacked in series, and each pair included two parallel washers, such that the resisting load is doubled compared with the case of W8 while the deformation capacity is unchanged. No grease was applied to the SMA washers such that friction could exist for those stacked in parallel. Details of the test specimens are summarised in Table 1 with the symbols explained in Fig. 1(a).

3.2 Test setup, instrumentation, and loading procedure

The test setup was designed such that the specimens acted as typical cantilever sub-frames. As shown in Fig. 2(a), the steel column was placed vertically with the two ends fixed to the girders of the reaction frame. The steel beam was connected to the column via the connection zone, and the cyclic load was applied onto the steel beam at a distance of L_r =1025 mm (i.e., lever arm) from the column face by a double acting hydraulic load jack. A hinge was used at the loading head to ensure that the cyclic load was appropriately transferred to the end of the beam with no secondary moment induced. The load was directly read by a load cell attached to the load jack. Although the considered test arrangement may be different from the actual scenario where the column inclines during earthquakes, it is believed that the key properties of the connections can be sufficiently reflected.

Fig. 2(b) shows the instrumentation arrangement for the specimens. The strain development of each bolt was measured by a pair of longitudinal strain gauges mounted on two opposite sides of the bolt shank. These strain gauges were mainly used for monitoring the level of the applied bolt

preload. More strain gauges were placed at the end-plate, beam stiffeners, and beam flanges to check if these components experienced yielding during the loading process. The overall deformation of the specimens was monitored via a set of linear variable differential transformers (LVDTs). LVDTs 1 and 2 were used to measure the elongations of the SMA bolts, and the readings may also be conveniently converted to the bolt strain. LVDTs 3 and 4 were placed at the end-plate for obtaining the gap opening angle, i.e., concentrated rotation of the connection (θ_c). LVDTs 5 and 6 were located at the end of the internal HS bolts with the main purpose of bolt preload control. LVDT 7 was used to record the shear slippage between the end-plate and column face. The vertical displacement of the loading point (Δ) was measured by LVDT 8, and the drift can be calculated by $\theta = \Delta/L_r$.

A target pre-strain of 5000 με, corresponding to a preload of approximately 50% of the 'yield' strength (forward transformation stress), was applied to the SMA bolts prior to the cyclic test. However, for the 8 mm diameter and 290 mm long SMA bolts, a reduced pre-strain of 4000 με was applied, since a pre-strain beyond this value might cause damage to these slender SMA bolts due to an unfavourable twisting effect. For the internal HS bolts, the preload was applied by monitoring the LVDT readings of the bolt end. A 1 mm total pre-compression was considered for each HS bolt, corresponding to a 0.25 mm pre-compression for each individual SMA washer. This value of pre-compression would ensure that the SMA washer groups were reasonably tightened, while a sufficient deformability was still available. After the bolt preload procedure was finished, the cyclic load was applied following the SAC project recommendation [27], as schematically shown in Fig. 2(a). A maximum applied drift of 4% was considered in this study.

4. Test observations

4.1 General behaviour

The four specimens exhibited the anticipated deformation mode during the cyclic loading process. The rotation demand was provided by the gap opening between the end-plate and column face, which caused elongation of the SMA bolts and concurrently compression of the SMA washers. Being stacked with different combination patterns, the SMA washers deformed synchronously under

compression. The end-plate behaved as a 'thick plate', enabling a V-shape gap opening mode with insignificant bending of the end-plate itself. This means that the centre of compression was located in the vicinity of the upper or lower ends of the extended end-plate. After completion of the tests, the main structural members remained elastic, indicating minimal post-earthquake repair work necessary. In addition, the SMA bolts and washers stayed 'tightened', which implied that these key components were still functional and thus the connections might be well prepared for further earthquake excitations (e.g., aftershocks). No failure was observed for any member or component of the specimens by the end of the tests. The typical deformation shapes of the specimens are shown in Fig. 3.

4.2 Moment-rotation responses

The measured moment-drift curves of the specimens are given in Fig. 4. Obvious flag-shape hysteretic responses with negligible residual deformation are observed, where the hysteretic shape seems to be dependent on the arrangement of the SMA bolts and washers. The moment-drift curve first follows a linear response with insignificant hysteresis at 0.375% drift. This indicates that the initial deformation demand of the specimens is mainly provided by the elastic deformation of the steel members. Some specimens (D8L240 in particular) show a low stiffness response over a very short range of the initial loading stage, although the stiffness quickly regains with increase in load. With a careful inspection, it is deduced that this response might be caused by a non-perfect contact condition between the end-plate and the column face. Forward transformation of the SMA components, signified by recognizable hysteresis loops, is developed when 0.75%-1% drift is achieved, and afterwards more obvious hysteresis loops with increasing energy dissipation start to show. In addition, pronounced hardening is observed from 1% drift onwards, a phenomenon which could be attributed to the unique forward transformation and martensitic hardening characteristics of SMA. At 4% drift, the maximum moment (M_{max}) ranges between 10 kNm and 29 kNm, which depend on the bolt size and washer arrangement. It is worth mentioning again that the current specimens are proof-of-concept small-scale connections, while for practical applications, a higher moment

resistance is often required which can be readily achieved by increasing the size or number of the SMA components. The shear resistance of the SMA-WB specimens appears to be adequate with almost no shear slippage between the end-plate and the column face (the measured slippage is up to 0.5 mm).

From the perspective of ductility, Eurocode 8 [28] requires that the beam-to-column connections should be designed to provide a rotational capacity of no less than 0.035 radians for structures of Ductility Class High (DCH), and 0.025 radians for structures of Ductility Class Medium (DCM). According to AISC [29], the rotational capacities for Special Moment Frames (SMFs) and Intermediate Moment Frames (IMFs) are 4% and 2% inter-storey drifts, respectively. The ductility of the connections could be evaluated by constructing a skeleton curve based on the available moment-drift hysteretic response, where the rotational capacity is deemed to be reached when the moment resistance decreases to 85% of the ultimate moment. According to the moment-drift responses obtained for the current connections, no decrease of moment resistance is observed, and thus the rotational capacities of all the specimens are at least 4% drift. This indicates that the specimens satisfy the DCH and SMF criteria in terms of ductility.

4.3 Strain readings

The typical strain gauge readings of the specimens are shown in Fig. 5, and similar responses are observed for the other specimens. For the external SMA bolts, the strain values given by both the strain gauges and LVDTs are provided and compared in Fig. 5(a), where for the latter case the calculated strain was taken as the ratio of the bolt elongation (by LVDT) over the working/parallel bolt length. It can be seen that the strain gauge reading becomes unreliable beyond 2%, which could be due to their limited measurement range, as mentioned before. The results converted from the LVDT readings show that the bolt strain could exceed 0.04 at 4% drift. For the other specimens with shorter SMA bolts, the maximum bolt strain typically exceeds 0.05 (not shown in the figure). According to the coupon test results, these bolts were at the late forward transformation stage and were quite close to the martensitic finish strain at 4% drift. The strains of the SMA washers were not

explicitly measured, but the conditions of the washers could be indirectly reflected by the movement of the HS bolts. Based on the associated LVDT readings (not shown in the figure), the maximum compression (including pre-compression) per washer at 4% drift is approximately 1.5 mm. This indicates that the deformability of SMA washers was not fully consumed, recalling that the allowable compression per washer is 2.7 mm.

The strain gauge readings shown in Fig. 5(b) confirm that the steel beam stayed elastic during the entire loading procedure. As the beam flange strain is proportional to the applied moment, the shape of the strain-drift response is consistent with the moment-drift responses. Fig. 5(c) shows the longitudinal strain development condition at the upper and lower surfaces of the end-plate immediately near the beam stiffeners. A high level of local compressive strain is observed at these regions, which is believed to result from the significant thrust action from the beam stiffeners that acted as the centre of compression when the connection rotated. Being further away from the junction between the end-plate and the beam stiffeners, the strain gauges at the mid part of the beam stiffeners show decreased strain values, as shown in Fig. 5(d). Generally speaking, the strain gauge readings are coherent with the design intention that the inelastic deformation of the specimens is mainly offered by the SMA bolts as well as the SMA washers.

5. Further discussions on test results

5.1 Strength and stiffness

Strength and stiffness are two fundamental characteristics for beam-to-column connections. According to Eurocode 3 [30], the connections can be categorized in terms of their stiffness into rigid, semi-rigid, or nominal-pinned, as detailed in Table 3, through comparisons against the rigidity of the adjacent beams EI_b/L_b, where E = Young's modulus, I_b = second moment of area of the beam, and L_b = span of the beam. It should be noted that in the table, K_{ini} is the initial tangent stiffness obtained from the moment-concentrated rotation response rather than the moment-drift response. The results show that the considered specimens are all semi-rigid connections, although specimen D12L290W8, with $K_{ini}/(EI_b/L_b) > 8$, may be considered as a rigid connection when employed in a non-sway bracing

frame [30]. In addition, the stiffness of specimen D8L240W16 is more than twice of that of specimen D8L240, indicating that the SMA washers have positive contribution to the connection stiffness. The low initial stiffness of specimen D8L240 could also be caused by the non-perfect contact condition between the end-plate and the column face, as mentioned before. It is worth mentioning that semi-rigid/partially-restrained connections are not considered in the current AISC standard for prequalified connections for special and intermediate moment frames [31], and therefore rigid connections are recommended in practical design. The connection stiffness can be increased by increasing either the preload or the size of the SMA components, as will be explained later in Section 7.

On the other hand, beam-to-column connections can be alternatively classified into full-strength, partial-strength, or nominal-pinned connections in terms of their strength, where the detailed criterion is provided in Table 3. Specimens D8L240 and D8L290W8, with M_{max}<0.20$M_{b,pl}$, can be generally considered as nominal-pinned connections. It is believed that the relatively small moment resistance is due to the small size of the SMA bolts (diameter = 8 mm) used for the specimens. Increasing either the bolt diameter or the number of washers stacked in parallel could effectively increase the moment resistance, and as a result, specimen D12L290W8 fall into the category of partial-strength connections. It should be kept in mind that in practice, the self-centring connections are preferably designed as partial-strength connections such that the potential damage to beams and columns could be minimal during earthquakes. The optimal $M_{max}/M_{b,pl}$ ratio should be determined based on system-level analysis, which is not the focus of this study.

5.2 Energy dissipation

The flag-shape hysteresis exhibited by the specimens indicates a good level of energy dissipation. For each complete cycle, the dissipated energy (energy loss) W_D can be calculated by the total area encircled by that cycle. The values of W_D at varying drifts are given in Fig. 6(a), and for each drift level, the mean value of W_D from different cycles was taken. As shown in the figure, W_D stays at a very low level prior to 1% drift, a phenomenon which echoes the moment-drift responses that exhibit unrecognizable hysteretic loops at early loading stages. After 1% drift, the SMA

components advance into the forward transformation stage, and as a result W_D gradually increases with increase in drifts. At 4% drift, the maximum energy dissipation per cycle could achieve 0.6 kJ. Importantly, the presence of the SMA washers has significant contribution to energy dissipation. Compared with specimen D8L240, the value of W_D for specimen D8L240W16 at 4% drift is increased by more than 50%. In addition, the size of the SMA bolt is also shown to have a significant influence on energy dissipation, and, clearly, this is due to the larger moment resistance provided by the larger diameter SMA bolts.

An alternative indicator for energy dissipation capacity is equivalent viscous damping (EVD), which is expressed by:

$$EVD = \frac{W_D}{4\pi W_E} \tag{1}$$

where W_E is the energy absorbed in a linear system that has the same maximum deformation and maximum moment as those identified from the moment-drift curves. A higher EVD often means a more 'plump' hysteretic shape, and hence a higher energy dissipation capacity. As shown in Fig. 6(b), the EVD is below 5% at drifts up to 1%. With more recognizable hysteresis being observed beyond 1% drift, the EVD starts to increase. At 4% drift, the maximum EVD observed for the specimens exceeds 13%.

5.3 Self-centring ability

Due to the recoverability of the SMA bolts and SMA washers, the specimens exhibit excellent self-centring response with negligible residual rotation by 4% drift. According to the FEMA P-58-1 guideline [32], all the tested connections satisfy the Class DS1 criterion (the most strict class) which requires that the residual drift does not exceed 0.2% to ensure that 'no structural realignment is necessary for structural stability, but the building may require adjustment and repairs to non-structural and mechanical components'. The self-centring ability of the specimens may be further assessed by examining the moment resistance upon completion of the reverse transformation during the unloading process. This moment is called restoring moment M_{rst}, as illustrated in Fig. 6(c), where a positive M_{rst}

means no residual deformation, whereas a negative value indicates development of residual deformation. It is preferred that M_{rst} should, on one hand, be suitably high to allow adequate self-centring tendency promoted by the connections, but on the other hand, be reasonably low to ensure sufficient energy dissipation.

As shown in Fig. 6(c), the restoring moments of the specimens follow a descending trend with increase in drifts, but the values are always above zero, showing a reliable self-centring behaviour. The gradual decrease of M_{rst} might be explained by the minor degradation of the reverse transformation plateau with increasing deformation demand. This is known as Transformation Induced Fatigue (TIF), which is a commonly observed phenomenon exhibited by SMA. TIF is caused by microstructural changes when the peak strain advances beyond the elastic regime, and it is responsible for the degradation of the hysteretic response with increase in number of cycles, especially in the first few cycles. It is noted that TIF is different from 'conventional' structural fatigue under high cyclic loads. The results also show that the specimens with the same SMA bolt diameter (8 mm) exhibit a similar trend of M_{rst}, which implies that the self-centring ability of the connections is largely dependent on the performance of the SMA bolts. For specimen D12L290W8, where an increased bolt diameter is employed, the values of M_{rst} are increased, although the trend is still the same. At 4% drift, the M_{rst}/M_{max} ratio of the specimens ranges between approximately 5% and 12%, which could be an appropriate range for balance between self-centring ability and energy dissipation.

6. Numerical investigation

6.1 Modelling strategy

Following the experimental programme, a numerical investigation was conducted to enable a further understanding of the cyclic behaviour of the proposed SMA-WB connections. The models were built in the general finite element (FE) analysis programme ABAQUS [33]. Except for the SMA bolts and washers which were modelled using the 8-node linear brick elements C3D8, the remaining part of the model was discretized by the 8-node linear brick elements with reduced integration and hourglass control, i.e., C3D8R in ABAQUS nomenclature. Hard contact with a consistent friction

coefficient of 0.3 was defined for all the contact surfaces, and tie interactions were considered for all the welded junctions. The preloading process for the SMA bolts and washers was well simulated in the model, which was followed by the application of the cyclic load with the loading protocol similar to that used in the tests, but with only one loading cycle per drift level. For computational efficiency, a half model with an appropriate 'symmetry' boundary condition was established, as typically shown in Fig. 7.

For steel material, a kinematic hardening model with the von Mises yield criterion was used. The material properties, including the Young's modulus, yield strength, and ultimate strength, were obtained from the tension coupon tests. As for the SMA, a built-in Auricchio's material model [34] was adopted to simulate the superelastic effect of SMA under isothermal conditions. The key material parameters include transformation stresses (σ^{Ms}, σ^{Mf}, σ^{As}, and σ^{Af}), Young's moduli (E^A and E^M), maximum transformation strain ε_L, and Poisson ratios (ν^A and ν^M). Based on the typical coupon test results of the 8 mm diameter SMA bolts, the basic material properties for the SMA bolts are extracted, as summarised in Table 4 with key symbols explained in Fig. 7. As no direct material test was conducted for the SMA washers, the material parameters for the SMA bolts were representatively used for the washers. While the size effect and variations in manufacturing processes could be sources of discrepancy, this assumption might be reasonable as the washers and bolts were made by the same manufacturer using the same chemical composition.

6.2 Validation and discussion

Adopting the considered modelling strategy, the FE models were established and verified against the test results. As the material tests were performed on the 8 mm-diameter SMA bolts, only the D8 series specimens were selected for FE modelling. As shown in Fig. 7, the predicted deformation mode agrees well with the test observation. At large drifts, the SMA bolts further away from the centre of compression elongate due to gap opening, and concurrently the SMA washer groups are compressed significantly. The FE results also confirm that the beam, column, and end-plates stay elastic, although minor plastic deformations are developed at the end-plate and beam

stiffener junction which acts as the centre of compression. This is also closely coherent with the strain gauge readings.

The test and FE predicted moment-concentrated rotation responses are compared in Fig. 8. Satisfactory agreements are observed, although the predicted loading and unloading curves do not exactly match the test curves. The discrepancy may be explained by the following reasons: 1) the column face and the end-plate are ideally flat in the FE model, and therefore, the initial low stiffness response due to the non-perfect contact condition observed in some specimens is not exhibited in the FE model. As a result, The FE models tend to provide larger initial stiffness compared with the test results, especially for specimen D8L240; 2) transformation induced fatigue (TIF) of SMA was not considered in the FE model, leading to an overestimation of the restoring moment (M_{rst}), especially at large drifts; and 3) the possible deviation of material properties in different SMA components was ignored in the current FE models that adopt a consistent SMA material property. Nevertheless, the flag-shape hysteretic performance of the connections at various drift levels is adequately captured, and the influence of varying test parameters is sufficiently reflected.

The satisfactory agreement enables a further numerical study to be conducted looking into some parameters that were not considered in the test program. Considering a typical specimen (i.e., D8L290W8), the influence of the washer pre-compression is illustrated in Fig. 9(a). Compared with the reference case where a 0.25 mm pre-compression is applied to each SMA washer, an increased pre-compression of 1 mm is shown to cause evident increases in the initial stiffness and decompression moment of the connection. In addition, the SMA washers with increased pre-compression still have sufficient deformability to accommodate the 4% target drift. It is recalled that each washer can offer a deformation ability of 2.7 mm, and accordingly, only around 1.5 mm needs to be consumed in order to achieve 4% drift. In other words, the remaining deformation ability, i.e., 1.2 mm per washer, can be used for pre-compression. The above result suggests that in practical design, the SMA washers are preferably tightened with a sufficiently large pre-compression to benefit the connection stiffness, although an upper limit should be determined depending on the required

deformability of the connection. Similarly, an increased preload for the SMA bolts also improves the connection stiffness, as illustrated in Fig. 9(b). It should be noted that too slender SMA bolts should be avoided in practice due to the unwanted twisting effect during the actual tightening procedure.

7. Design considerations

The design moment-rotation characteristic of a connection can be simplified by a linearized approximation, where a bi-linear response is one of the most widely considered codified simplifications. The basic characteristics such as strength and stiffness need to be determined for regular bi-linear design of the connection. According to the test and numerical results presented above, it is seen that the overall performance of the SMA-WB connections largely depends on the behaviour of individual SMA bolts and washers. The performance is also influenced by the preloading condition of these components. Building on the 'component-based' design framework given in Eurocode 3 [30], the design strength and stiffness of the SMA-WB connections can be predicted using the design procedure described as follows.

The design strength (i.e., design yield moment resistance) of a SMA-WB connection is contributed by the moment of forces provided by the SMA bolt and washer rows in relation to the centre of compression. The test results indicate that the centre of compression is in the vicinity of the upper or lower extremes of the extended end-plate that is designed conforming to the 'thick-plate' criterion [35]. Assuming a V-shape gap opening mode, the design yield moment resistance $M_{y,Rd}$ can be calculated by [30]:

$$M_{\mathrm{y},Rd} = \sum_i F_{b,y} h_i + \sum_j F_{\mathrm{w},y} h_j \tag{2}$$

where $F_{b,y}$ is the total yield resistance of each SMA bolt row, $F_{w,y}$ is the total yield resistance of each SMA washer row, and h_i and h_j are the distances from the SMA bolts and SMA washers to the centre of compression, respectively, as marked in Fig. 1(a).

The yield resistance of SMA bolts is easily calculable by multiplying the design forward transformation stress σ^{Ms} by the shank area A_b. For the SMA washers, the theoretical elastic solution for normal Belleville washers can be adopted, as detailed in the relevant handbook [36]. It is

recommended that the state of a washer can be monitored by the stress level at a reference location (point OM as marked in Fig. 1(a)), and it is often assumed that $F_{w,y}$ is achieved when the stress at this location (σ^{OM}) reaches σ^{Ms}. It should be noted that point OM is a typical high stress zone rather than the peak stress location. Selecting the peak stress location for determining $F_{w,y}$ can lead to a significant underestimation of $F_{w,y}$. The development of the critical stress σ^{OM} is expressed by [36]:

$$\sigma^{OM} = -\frac{12ETs}{\left(1-\mu^2\right)K_1 D_e^2 \pi} \tag{3}$$

$$K_1 = \frac{\left(\left(\delta-1\right)/\delta\right)^2}{\pi\left(\left(\delta+1\right)/\left(\delta-1\right)-2/\ln\delta\right)},\ K_2 = \frac{6\left(\left(\delta-1\right)/\ln\delta-1\right)}{\pi\ln\delta},\ K_3 = \frac{3\left(\delta-1\right)}{\pi\ln\delta} \tag{4}$$

where s is the compressive deformation of the washer, E is Young's modulus of the SMA material, μ is Poisson's ratio which is taken as 0.33, $\delta = D_e/D_i$, and the other symbols related to the geometric dimension are illustrated in Fig. 1(a). Considering the representative material properties shown in Fig. 7, the corresponding compressive deformation s upon yielding of the washer can be deduced, i.e., s = 0.66 mm. With the obtained yielding deformation, the yield resistance $F_{w,y}$ of the individual SMA washer can be obtained by [36]:

$$F_w(s) = \frac{4ET^3 s}{\left(1-\mu^2\right)K_1 D_e^2}\left[\left(\frac{H_0}{T}-\frac{s}{T}\right)\left(\frac{H_0}{T}-\frac{s}{2T}\right)+1\right] \tag{5}$$

where H_0 is the maximum deformation capacity of each washer. As for the design stiffness $S_{ini,\eta}$ of the SMA-WB connection, the following equation employing the principle of the component-based design approach is employed:

$$S_{ini,\eta} = \sum_i \frac{F_{b,y}EA_b}{\left(F_{b,y}-F_{b,pre}\right)L_p}h_i^2 + \sum_j \frac{F_{w,y}k_w}{\left(F_{w,y}-F_{w,pre}\right)}h_j^2 \tag{6}$$

where L_p is the working length of the SMA bolts, and k_w is the stiffness of the considered SMA washer group. The stiffness of each individual SMA washer can be calculated by Eq. (5), and when the washers are stacked with various combinations, the value of k_w should be adjusted accordingly. In addition, Eq. (6) enables the consideration of preload, where $F_{b,pre}$ and $F_{w,pre}$ are the preloads applied onto the SMA bolts and SMA washers, respectively. The inclusion of bolt preload tends to increase

the design stiffness of the connection, and when the preload equals to the yield resistance, the design stiffness can be considered as infinite prior to decompression.

Based on the design strength $M_{y,Rd}$ and design stiffness $S_{ini,\eta}$, a simplified bi-linear moment-rotation response can be constructed, as illustrated in Fig. 8. It is seen that the design predictions of the two quantities agree well with the FE and test results. In particular, the design stiffness $S_{ini,\eta}$ adequately reflects the 'secant' connection behaviour which forms the basis on the simplified bi-linear design moment-rotation characteristic for elastic-plastic global analysis [30]. The design strength $M_{y,Rd}$ is also quite accurate, although the hardening response exhibited in the specimens is not taken into account. It seems that the significance of hardening depends on the number of the SMA washers, because these washers could have an evident hardening response, as confirmed in Fig. 1(b).

A simple example is given here to further illustrate the design of such self-centring connections for a "real" building. The prototype steel frame is a 5-storey, 4×3 bay office building (located at ground type B soil) designed by Dimopoulos et al. [37] according to Eurocode 8 [28]. The typical plan and elevation views of the building are shown in Fig. 10(a). The yield strengths for the steel beams and steel columns are 300 MPa and 350 MPa, respectively. An internal beam-to-column (strong-axis) connection on the third floor (as marked in the figure) in the prototype steel frame building is selected and modified for the illustration of the connection design.

As currently there is no codified recommendation available for designing SMA-WB connections, the following rules are preliminarily considered: 1) the design initial stiffness of the SMA-WB connection is comparable to the rigid connection criterion such that the building has sufficient lateral stiffness against normal loading conditions, e.g., wind; 2) the 'yield moment' of the SMA-WB connection is taken as less than 80% of the yield moment resistance ($M_{b,el}$) of the steel beam (IPE400) in order to ensure that inelastic deformation first occurs in the connection while the steel beam is still elastic; 3) the SMA components (SMA washers in particular) are designed to provide a concentrated rotation capacity of at least 0.03 radians, corresponding to an inter-storey drift of approximately 0.04 radians; 4) the connection is expected to exhibit over-strength beyond the yield

moment; which means that a certain level of beam yielding is allowed at large inter-storey drifts. Other necessary design parameters for SMA are: forward transformation start stress = 350 MPa, and Young's modulus of SMA = 35 GPa. These are quite typical values according to the existing studies on large-scale SMA bars/bolts [13-16].

Based on the basic design rules, a "real-scale" SMA-WB connection is designed, as illustrated in Fig. 10(b). The connection consists of four SMA bolt rows (two upper bolt rows and two lower bolt rows) to provide an adequate level of moment resistance. This arrangement makes a total of eight SMA bolts to be used for the entire connection, where the shank diameter of each SMA bolt is 18 mm and the working/parallel length (L_p) is 380 mm. In addition, a total of eight M20 HS bolts, which are used in conjunction with SMA washer groups, are employed for the internal bolt rows. For each HS bolt, eight pairs of washer set are stacked in series, and each pair includes two parallel washers. The size of the SMA washers is the same as that considered for the test specimens. The centre of compression for the connection is assumed to be located at the end of the stiffened extended end-plate. All the other components (e.g. stiffeners) are appropriately designed.

Based on the considered geometric configuration and according to Eqs. (2) through (5), the calculated design yield moment resistance $M_{y,Rd}$ of the connection is 253 kNm, which is approximately $0.73M_{b,el}$. It should be noted that the contribution of moment resistance from the SMA bolts and washers closer to the centre of compression is conservatively neglected in the calculation of $M_{y,Rd}$. In order to achieve sufficient initial stiffness, relatively large preloads are applied to the SMA components. For both SMA bolts and washers, the preload is taken as 80% of their design yield resistance. As a result, the design initial stiffness $S_{ini,\eta}$ of the SMA-WB connection is 195,853 kNm/rad according to Eq. (6). This value corresponds to $33EI_b/L_b$, which indicates that the connection can be considered as a rigid connection according to Eurocode 3[30]. From a deformability point of view, the peak strain (including prestrain) of the SMA bolts at 0.03-radian concentrated connection rotation is 6%, and at the meantime, the peak compressive deformation (including pre-deformation) of each individual SMA washer is 2.6 mm. This confirms that the connection can provide a

concentrated rotation of at least 0.03 radians. It is worth mentioning that a more efficient design may be achieved by optimising the geometric configuration of the SMA washers.

8. Summary and conclusions

An innovative type of self-centring connection, namely, a hybrid self-centring connection with HS bolts, SMA Belleville washers, and SMA bolts (SMA-WB connection), has been presented in this paper. The moment resistance of the connection is provided by the SMA bolts and the SMA Belleville washers while the shear resistance is provided by the high strength bolts. The study commenced with an introduction of the two basic SMA elements, i.e., SMA Belleville washers and SMA bolts, used for the connection, and after understanding their fundamental mechanical characteristics, four proof-of-concept connections were tested, considering bolt dimension and washer arrangement as the main parameters. A numerical investigation was subsequently performed to enable a more in-depth understanding of the connection behaviour, and a design model was finally developed. The main findings and conclusions are noted as follows.

- The individual SMA washers showed good self-centring ability, cyclic loading repeatability, and energy dissipation capacities. The satisfactory performance also highlighted the importance of appropriate geometric design for these washers. In addition, a controlled D_3/D_1 ratio ranging from 1.25 to 1.30 led to good ductility of the SMA bolts.
- The SMA-WB connections exhibited the anticipated deformation mode during the cyclic loading process. The rotation demand of the connection was provided by the gap opening between the end-plate and the column face, which was accompanied by elongation of the SMA bolts and concurrently compression of the SMA washers.
- According to the measured initial stiffness, the specimens could be generally categorised as semi-rigid connections. From the perspective of strength, the specimens were nominal-pinned or partial-strength connections, and it was found that increasing either the bolt diameter or the number of washers stacked in parallel could effectively increase the moment resistance.

- The SMA-WB connections exhibited very good ductility which satisfies the criteria of Ductility Class High (DCH) and Special Moment Frame (SMF) required by Eurocode 8 [28] and AISC [29], respectively. The energy dissipation ability was found to be moderate with a maximum EVD of approximately 13.5%.
- The presence of the SMA washers had evident contributions to strength, stiffness, and energy dissipation, and the follow-up numerical study shows that increasing the preload levels of either the SMA washers or SMA bolts could improve these properties, especially stiffness.
- Building on the 'component-based' design framework given in Eurocode 3 [30], a design model which enables an idealised bi-linear description of the moment-rotation responses of SMA-WB connections was finally proposed and was found to agree reasonably well with the test results and FE predictions.

From the cost point of view, although the unit price of SMA is still relatively high compared with other constructional materials, SMA is only used in critical areas of a structure in small amounts, and massive order may further decrease the unit cost. As the material price decreased significantly over the past decade, it is reasonable to expect further room for price concession in the foreseeable future with continuously improved metallurgic technologies. The excellent corrosion resistance also makes SMA economically viable from a life-cycle design point of view.

9. Acknowledgements

The financial supports from the Natural Science Foundation of China (NSFC) with Grant Nos. 51778456 and 51408437 are acknowledged. Partial funding supports received from The Hong Kong Polytechnic University (Project No. G-YL86) and the Chinese National Engineering Research Centre for Steel Connection, The Hong Kong Polytechnic University (Project No. 1-BBYQ) are also acknowledged.

References

[1] Sultana P, Youssef MA. Seismic performance of steel moment resisting frames utilizing superelastic shape memory alloys. Journal of Constructional Steel Research 2016; 125:239-51.

[2] McCormick J, Aburano H, Ikenaga M, Nakashima M. Permissible residual deformation levels for building structures considering both safety and human elements. Proc. 14th World Conf. Earthquake Engineering, Seismological Press of China, Beijing, 2008.

[3] Rinaldin G, Amadio C, Fragiacomo M. Effects of seismic sequences on structures with hysteretic or damped dissipative behaviour, Soil Dynamics and Earthquake Engineering 2017; 97: 205-15.

[4] Qiu CX, Zhu SY. High-mode effects on seismic performance of multi-story self-centering braced steel frames. Journal of Constructional Steel Research 2016; 119:133-43.

[5] Wolski M, Ricles JM, Sause R. Experimental study of a self-centering beam-column connection with bottom flange friction device. Journal of Structural Engineering ASCE 2009; 135(5):479-88.

[6] Zhang AL, Zhang YX, Li R, Wang ZY. Cyclic behavior of a prefabricated self-centering beam–column connection with a bolted web friction device. Engineering Structures 2016; 111:185-98.

[7] Liew KM, Kitipornchai S, Ng TY, Zou GP. Multi-dimensional superelastic behavior of shape memory alloys via nonlinear finite element method. Engineering Structures 2002; 24(1): 51-7.

[8] DesRoches R, Taftali B, Ellingwood BR. Seismic performance of steel frames with shape memory alloy connections, part I – Analysis and seismic demands. Journal of Earthquake Engineering 2010; 14(4):471-86.

[9] Ma HW, Wilkinson T, Cho C. Feasibility study on a self-centering beam-to-column connection by using the superelastic behavior of SMAs. Smart Materials and Structures 2007; 16(5):1555-63.

[10] Fang C, Yam MCH, Lam ACC, Xie LK. Cyclic performance of extended end-plate connections equipped with shape memory alloy bolts. Journal of Constructional Steel Research 2014; 94:122-36.

[11] Yam MCH, Fang C, Lam ACC, Zhang YY. Numerical study and practical design of beam-to-column connections with shape memory alloys. Journal of Constructional Steel Research 2015; 104:177-92.

[12] Penar BW. Recentering beam-column connections using shape memory alloys. Master thesis, school of civil and environmental engineering, Georgia Institute of Technology, 2005.

[13] Speicher MS, DesRoches R, Leon RT. Experimental results of a NiTi shape memory alloy (SMA)-based recentering beam-column connection. Engineering Structures 2011; 33(9):2448-57.

[14] Wang W, Chan TM, Shao HL. Seismic performance of beam–column joints with SMA tendons strengthened by steel angles. Journal of Constructional Steel Research 2015; 109:61-71.

[15] Wang W, Fang C, Liu J. Self-centering beam-to-column connections with combined superelastic SMA bolts and steel angles. Journal of Structural Engineering ASCE 2017; 04016175.

[16] Wang W, Fang C, Liu J. Large size superelastic SMA bars: heat treatment strategy, mechanical property and seismic application. Smart Materials and Structures 2016; 25:075001.

[17] Fang C, Yam MCH, Lam ACC, Zhang YY. Feasibility study of shape memory alloy ring spring systems for self-centring seismic resisting devices. Smart Materials and Structures 2015; 24:075024.

[18] Wang W, Fang C, Yang X, Chen YY, Ricles J, Sause R. Innovative use of a shape memory alloy ring spring system for self-centering connections. Engineering Structures, submitted for review.

[19] Savi MA, Pacheco PMCL, Garcia MS, Aguiar RAA, Souza LFG, Hora RB. Nonlinear geometric influence on the mechanical behavior of shape memory alloy helical springs. Smart Materials and Structures 2015; 24(3):035012.

[20] Fang C, Wang W, He C, Chen YY. Self-centring behaviour of steel and steel-concrete composite connections equipped with NiTi SMA bolts. Engineering Structures 2017;150:390-408.

[21] Labrecque C, Braunovic M, Terriault P, Trochu F, Schetky M. Experimental and theoretical evaluation of the behavior of a shape memory alloy Belleville washer under different operating conditions. Proceedings of the annual Holm conference on electrical contacts, IEEE, Chicago, 1996.

[22] Maletta C, Filice L, Furgiuele F. NiTi Belleville washers: Design, manufacturing and testing. Journal of Intelligent Material Systems & Structures 2013; 24(6):695-703.

[23] Speicher M, Hodgson DE, DesRoches R, Leon RT. Shape memory alloy tension/compression device for seismic retrofit of buildings. Journal of Materials Engineering & Performance 2009; 18(5-6):746-753.

[24] Fang C, Zhou XY, Osofero AI, Shu Z, Corradi M. Superelastic SMA Belleville washers for seismic resisting applications: experimental study and modelling strategy. Smart Materials and Structures 2016; 25:105013.

[25] Tamai H, Miura K, Kitagawa Y, Fukuta T. Application of SMA rod to exposed-type column base in smart structural system. Proceedings of SPIE 5057, Smart Structures and Materials: Smart Systems and Nondestructive Evaluation for Civil Infrastructures, 2003.

[26] International Organization for Standardization (ISO). Metallic Materials — Tensile Testing–Part 1: Method of Test at Room Temperature, ISO 6892-1, London, British, 2009.

[27] Clark P, Frank K, Krawinkler H, Shaw R. Protocol for fabrication, inspection, testing, and documentation of beam-column connection tests and other experimental specimens, SAC Report SAC/BD-97/02, SAC Joint Venture, 1997.

[28] European Committee for Standardization (CEN). Eurocode 8: Design of structures for earthquake resistance–Part 1: General rules, seismic actions and rules for buildings, EN 1998-1, Brussels, Belgium, 2004.

[29] American Institute of Steel Construction (AISC). Seismic provisions for structural steel buildings, Chicago, 2010.

[30] European Committee for Standardization (CEN). Eurocode 3: Design of steel structures– Part 1-8: Design of joints, EN 1993-1-8, Brussels, Belgium, 2005.

[31] ANSI/AISC 358-10, Prequalified connections for special and intermediate steel moment frames for seismic applications, Chicago, Illinois, USA, 2010.

[32] Federal Emergency Management Agency, Seismic Performance Assessment of Buildings, Volume 1 – Methodology, FEMA P-58-1 / September 2012.

[33] ABAQUS Analysis User's Manual, ABAQUS Standard, Version 6.12, 2012.

[34] Auricchio F. A robust integration-algorithm for a finite strain shape-memory-alloy superelastic model. International Journal of Plasticity 2001; 17(7):971-90.

[35] Murray TM, Sumner EA. AISC Design Guide 4: Extended end-plate moment connections seismic and wind applications (Second Edition), 2003.

[36] Fromm E and Kleiner W. Handbook for disc springs, Schnorr Corporation, Hela Werbung, Heilbronn, 2003.

[37] Dimopoulos AI, Karavasilis TL, Vasdravellis G, Uy B. Seismic design, modelling and assessment of self-centering steel frames using post-tensioned connections with web hourglass shape pins. B. Earthq. Eng. 2013; 11(5): 1797-816.

List of figures:

List of tables:

Table 1 Basic details of specimens – measured values

	Bolt details						Washer details
Specimen designation	Total length L	Parallel length L_p	Shank diameter D_1	Threaded gross diameter D_2	Threaded net diameter D_3	No. of SMA washer per HS bolt	Washer arrangement
D8L290W8	290.5	226.2	7.97	12.40	10.04	4	×4 in series
D8L240W16	240.5	174.3	7.99	12.40	10.05	8	×2 in parallel ×4 in series
D12L290W8	290.5	225.5	11.75	18.90	15.55	4	×4 in series
D8L240	240.6	176.0	7.98	12.40	10.12	0	N/A

Table 2 Key steel material properties from coupon tests

Component	Young's modulus (GPa)	yield strength f_y (MPa)	ultimate strength f_u (MPa)
Beam flange	206.3	411.5	541.8
Beam web & stiffener	202.3	398.9	554.9
End-plate	197.7	408.0	556.2

Table 3 Stiffness and strength of connection specimens

Specimen	Stiffness			Strength		
	K_{ini} (kNm/rad)	$K_{ini}/(EI_b/L_b)$	Classification	M_{max} (kNm)	$M_{max}/M_{b,pl}$	Classification
D8L290W8	2958	3.72	Semi-rigid	12.9	0.17	Nominal-pinned
D8L240W16	3715	4.67	Semi-rigid	17.7	0.24	Nominal-pinned
D12L290W8	6828	8.59	Semi-rigid*	27.5	0.37	Partial-strength
D8L240	1788	2.25	Semi-rigid	9.5	0.13	Nominal-pinned

Note: For moment resisting frames: Rigid: $K_{ini}/(EI_b/L_b)>25$; Semi-rigid: $0.5< K_{ini}/(EI_b/L_b)<25$; Nominal-pinned: $K_{ini}/(EI_b/L_b)<0.5$;
For non-sway bracing frames: Rigid: $K_{ini}/(EI_b/L_b)>8$; Semi-rigid: $0.5< K_{ini}/(EI_b/L_b)<8$; Nominal-pinned: $K_{ini}/(EI_b/L_b)<0.5$;
For all frames: Full-strength: $M_{max}>M_{b,pl}$; Partial-strength: $0.25M_{b,pl}<M_{max}<M_{b,pl}$; Nominal-pinned: $M_{max}<0.25M_{b,pl}$.
*Rigid for non-sway bracing frames

Table 4 Material properties for simulation of SMA bolts

Material properties	Values
Forward transformation start stress σ_{Ms}	280 MPa
Forward transformation finish stress σ_{Mf}	380 MPa
Reverse transformation start stress σ_{As}	150 MPa
Reverse transformation finish stress σ_{Af}	75 MPa
Young's Modulus E_A	35 GPa
Young's Modulus E_M	25 GPa
Maximum transformation strain ε_L	5%
Poisson's Ratio ν_A	0.33
Poisson's Ratio ν_M	0.33

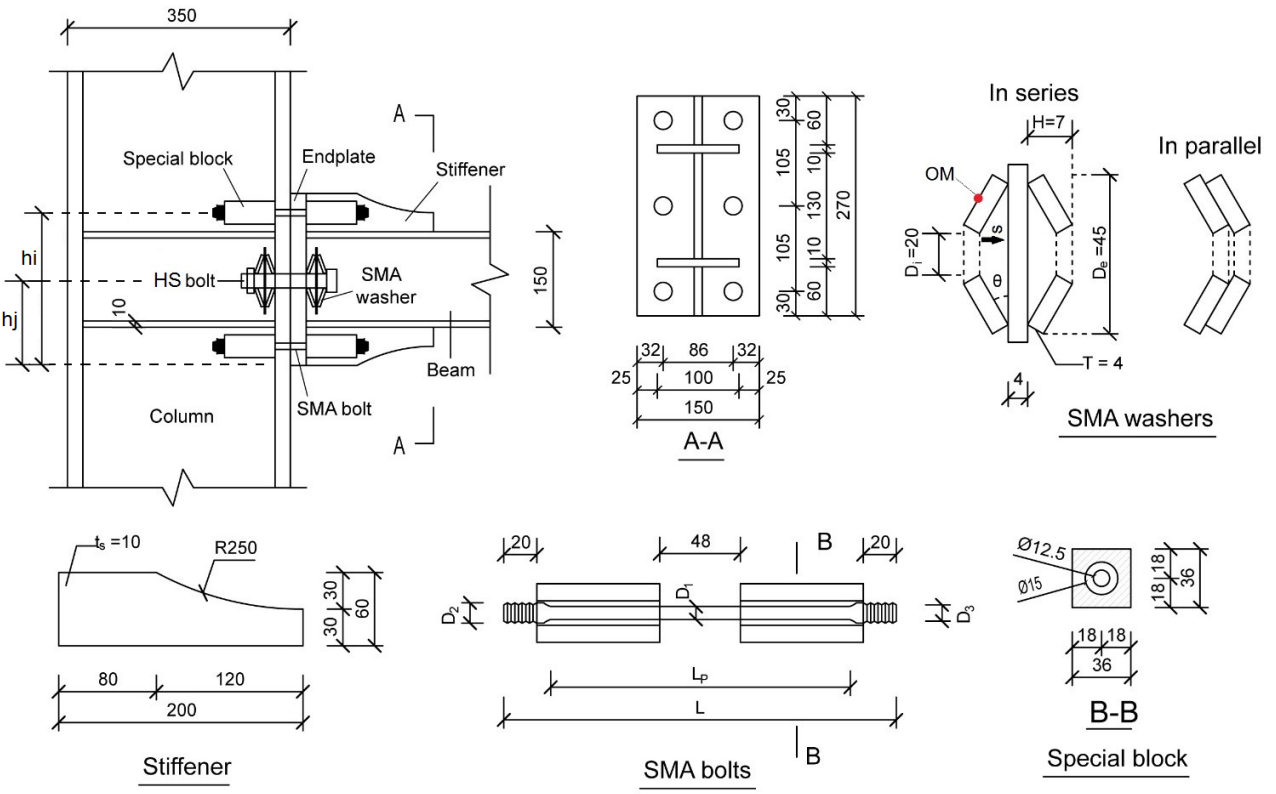

(a)

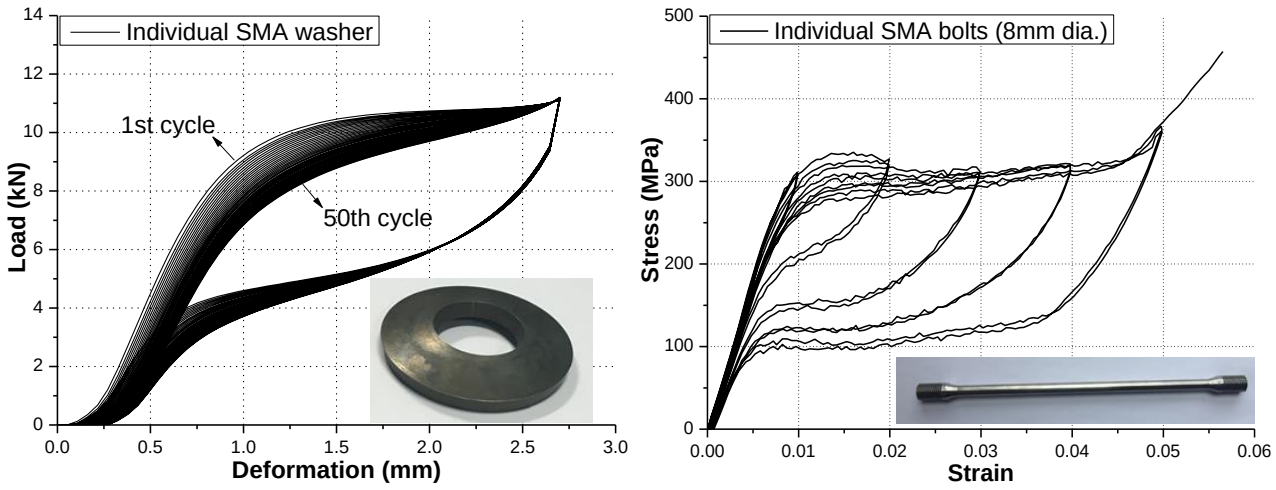

(b)

Fig. 1 Test specimens: a) geometric configurations and dimensions, b) material test results for SMA elements

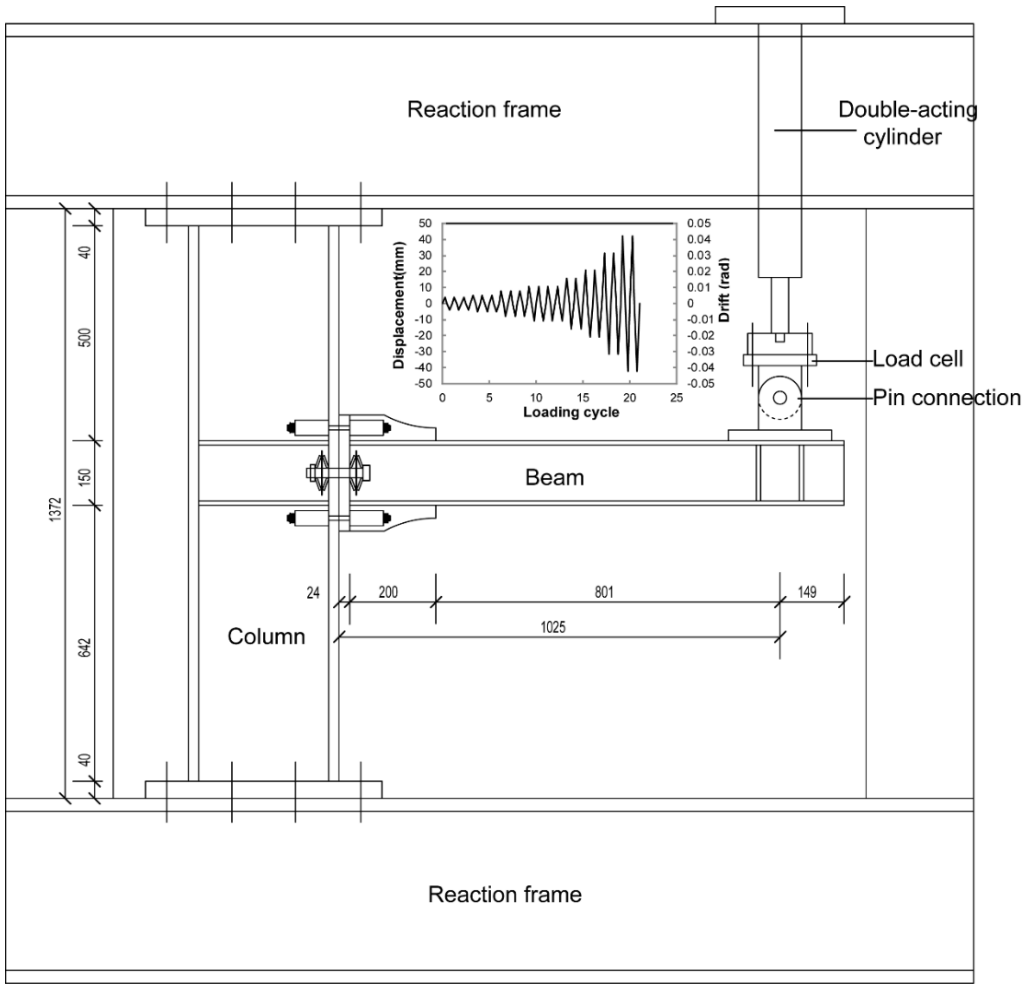

(a)

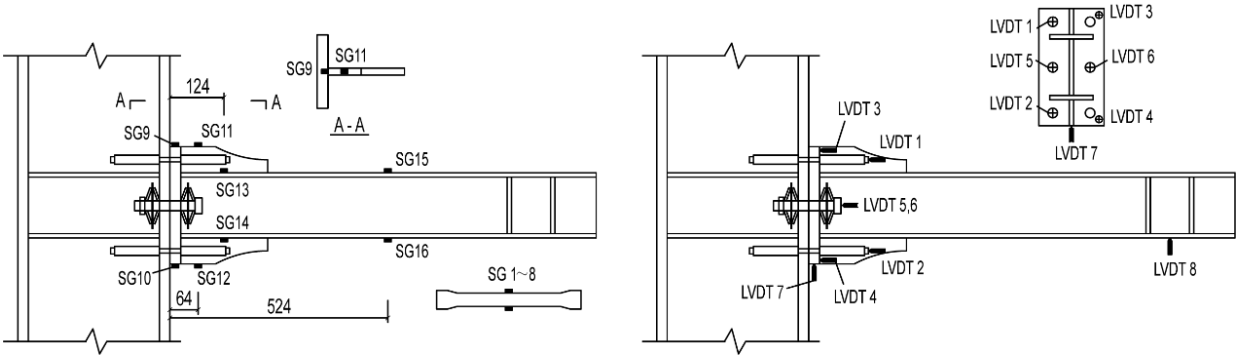

(b)

Fig. 2 Illustration of test arrangement: a) test setup, b) instrumentations

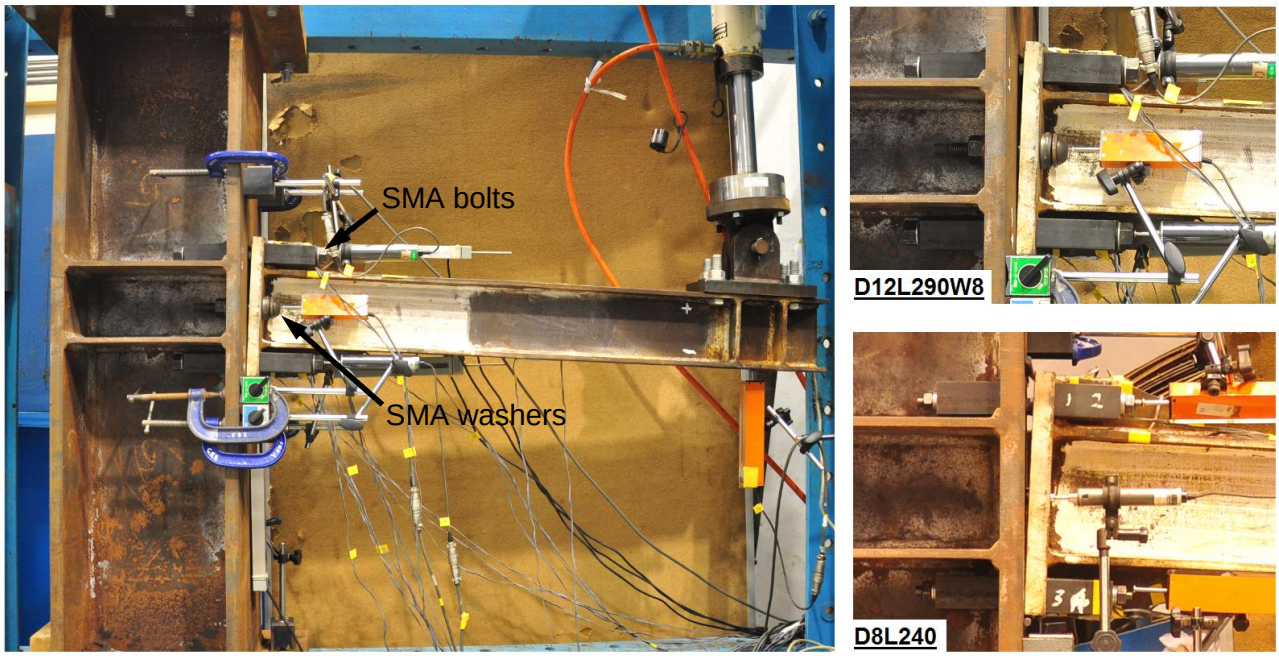

Fig. 3 Typical deformation modes of specimens

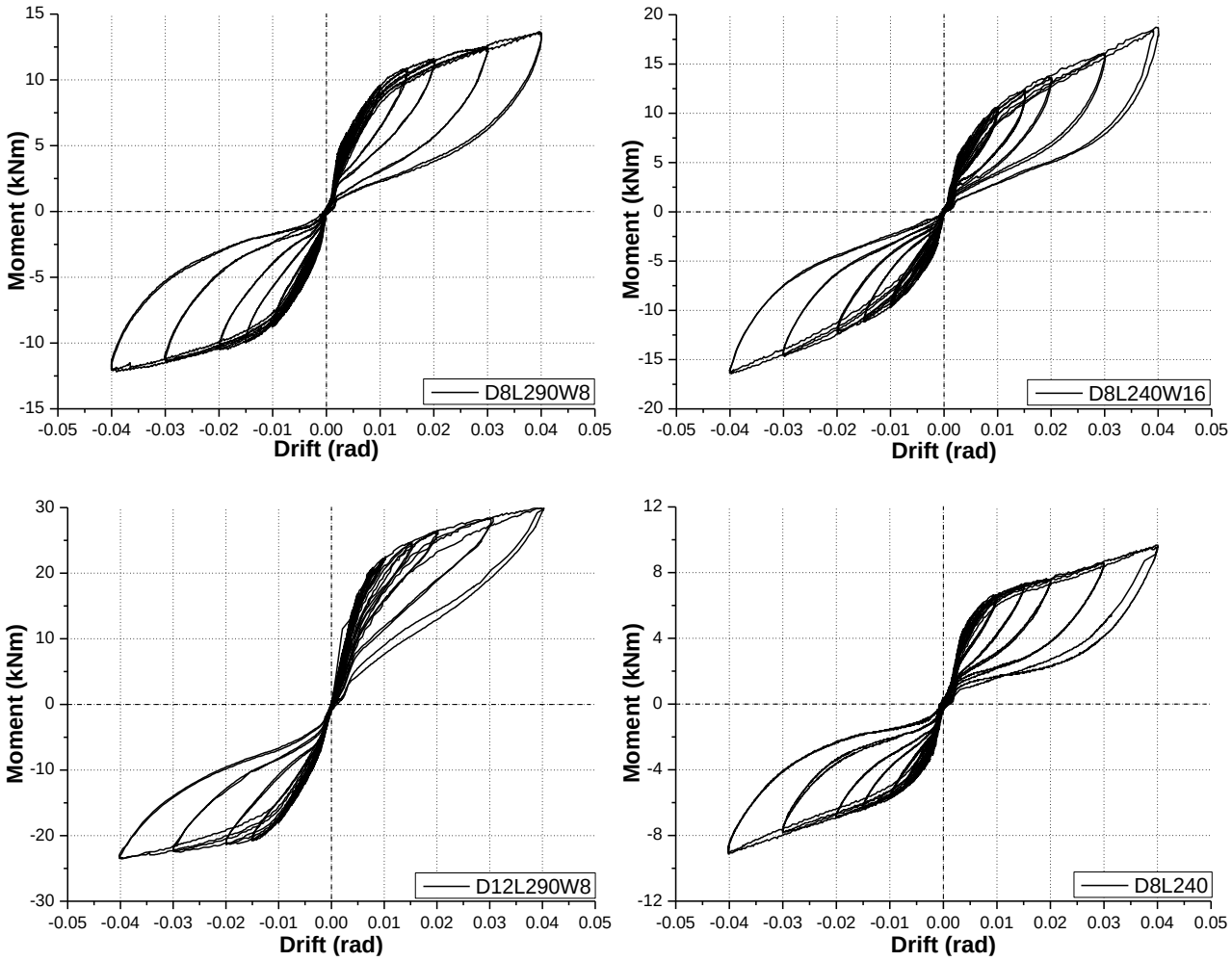

Fig. 4 Moment-drift responses of specimens

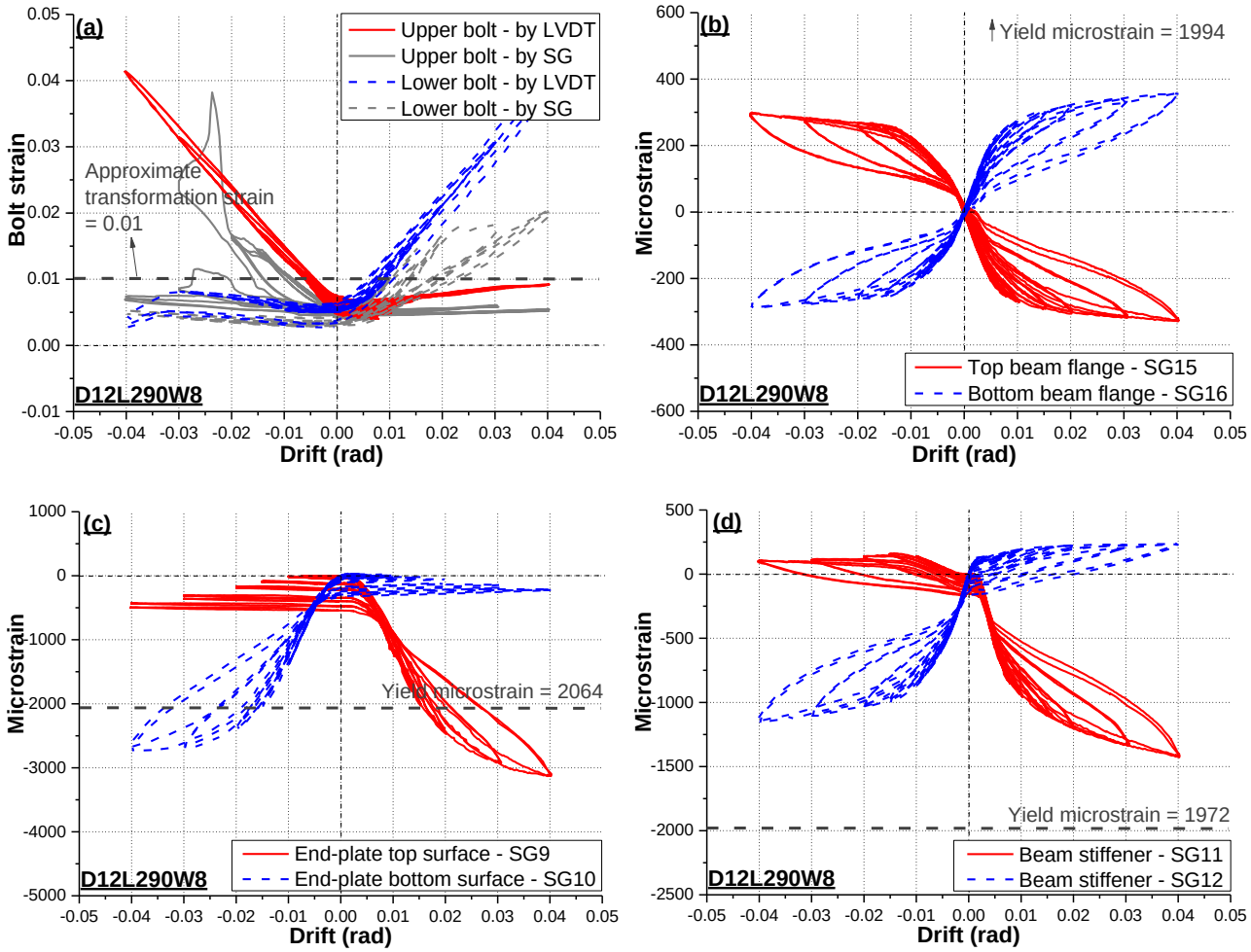

Fig. 5 Typical strain gauge readings at key locations (specimen D12L290W8)

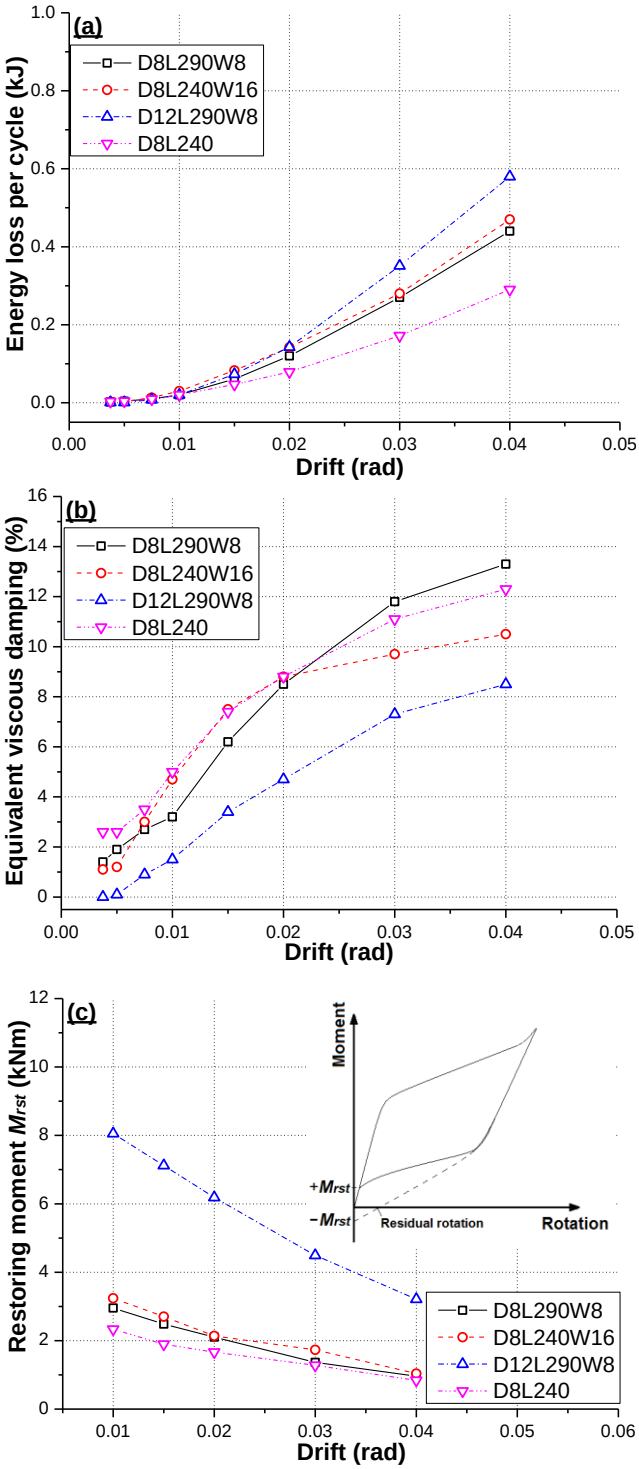

Fig. 6 Discussions of test results: a) energy loss per cycle, b) EVD, c) self-centring ability

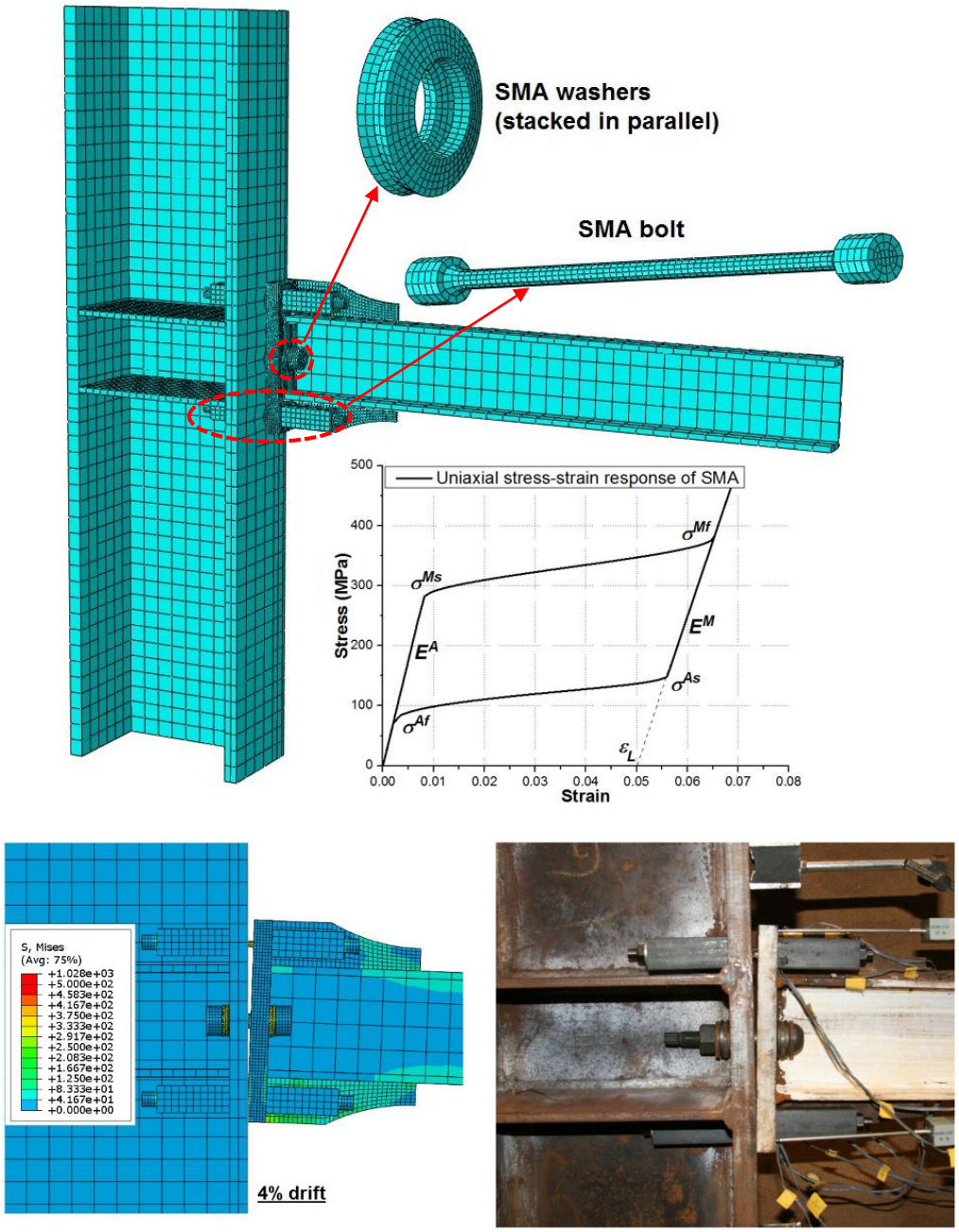

Fig. 7 Representative models and typical deformation mode (D8L290W8)

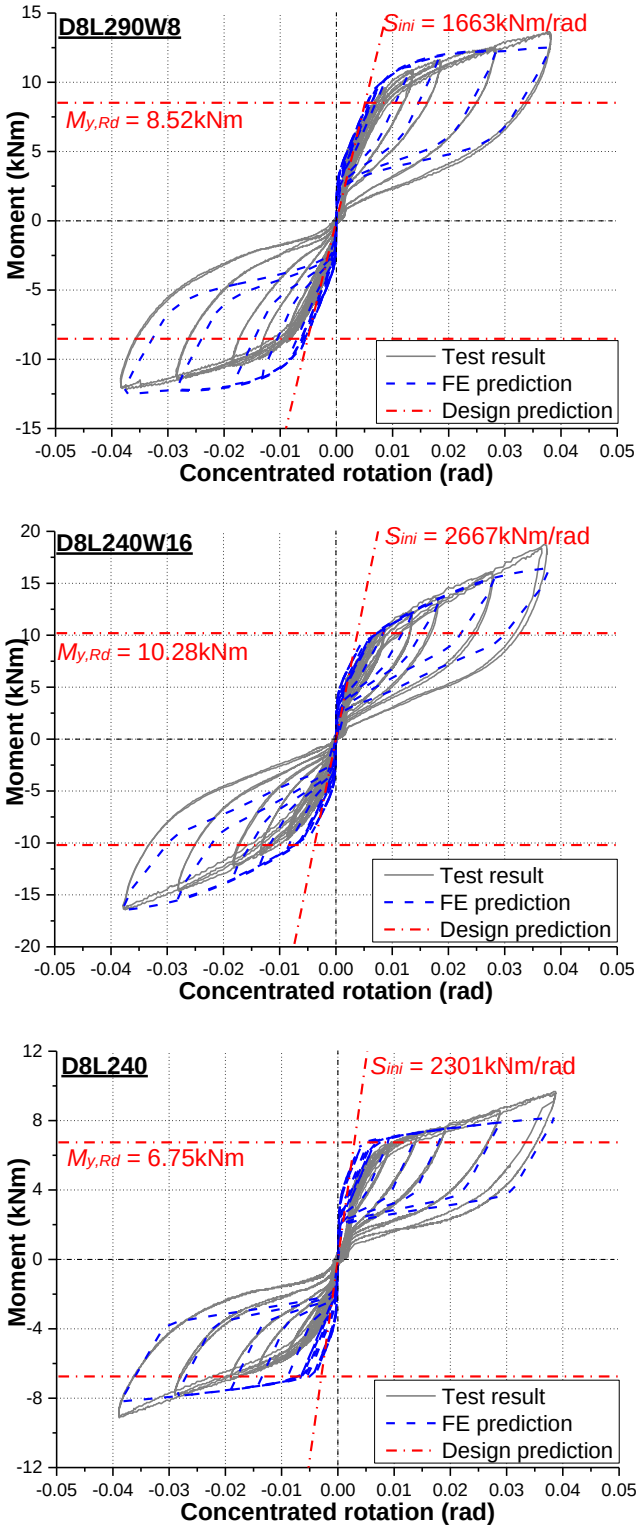

Fig. 8 Moment-concentrated rotation responses: FE predictions and design approximations

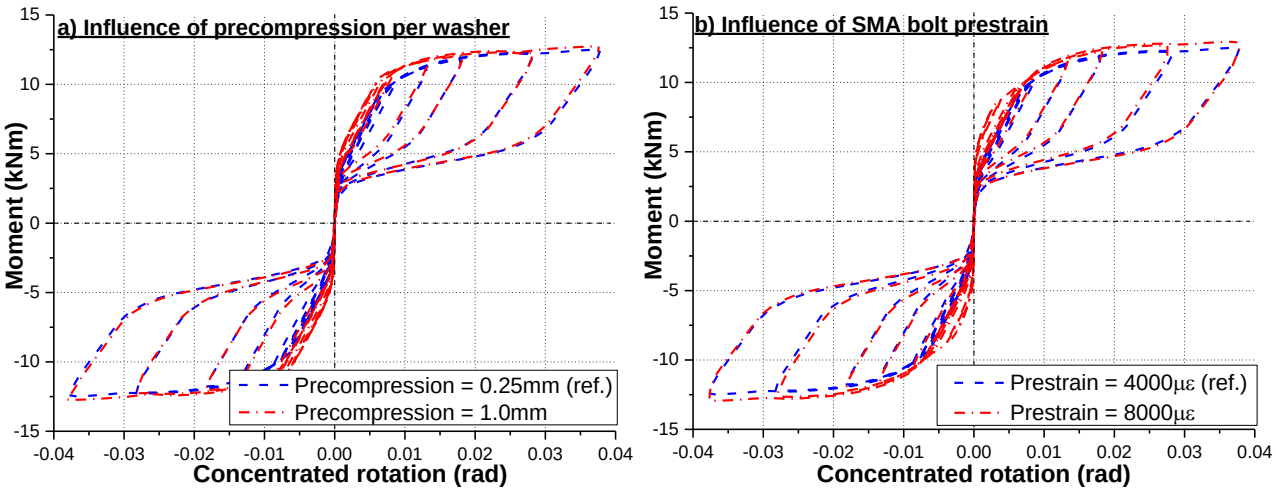

Fig. 9 Influence of preload of SMA components (D8L290W8)

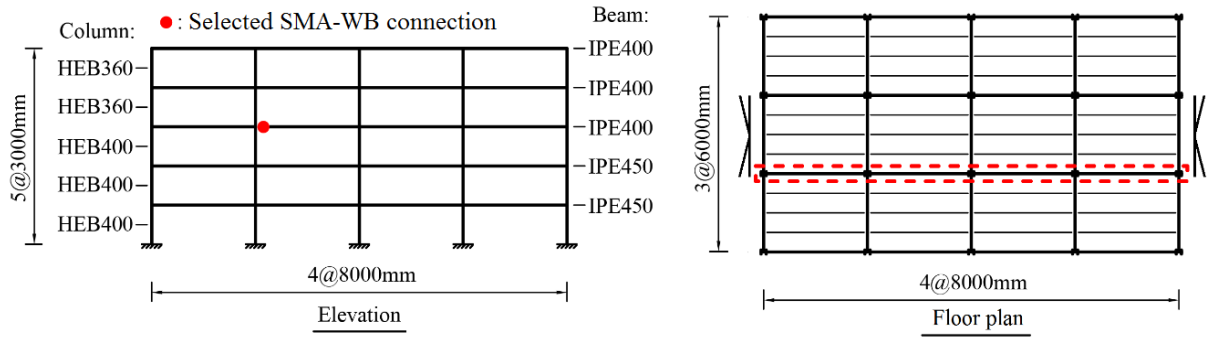

(a)

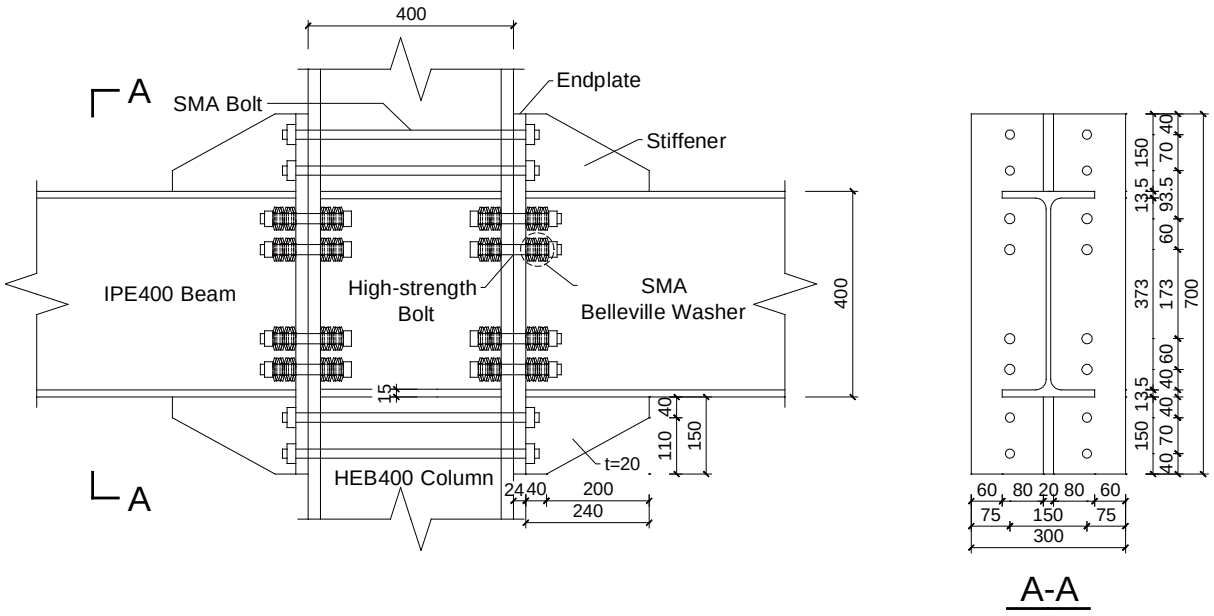

(b)

Fig. 10 Illustrative connection example: a) prototype building, b) connection detailing